

N 93 - 27571
317-37

Practical Limits to the Performance of Magnetic Bearings:

Peak Force, Slew Rate, and Displacement Sensitivity¹

163497
P-14

E. Maslen, Research Associate (1)
P. Hermann, Chief - Rotating Machinery
Research Mechanical (2)
M. Scott, Research Associate (1)
R. R. Humphris, Research Professor (1)

(1) Mechanical and Aerospace Engineering Department
Thornton Hall
University of Virginia
Charlottesville, VA

(2) Sundstrand Aviation Operations
4747 Harrison Ave.
Rockford, IL

Abstract

Magnetic bearings are subject to performance limits which are quite different from those of conventional bearings. These are due in part to the inherent nonlinearity of the device and in part to its electrical nature. Three important nonideal behaviors are presented: peak force capacity, force slew rate limitation, and sensitivity to rotor motion at large displacements. The problem of identifying the dynamic requirements of a magnetic bearing when used to support a known structure subject to known loads is discussed in the context of these limitations. Several simple design tools result from this investigation.

Introduction

Magnetic bearings are moving from the realm of science fiction into that of practical engineering. Not only is their feasibility being widely demonstrated, but many advantages over conventional bearings are becoming apparent. Amidst this atmosphere of optimism, it is important to recognize and understand the shortcomings of this class of devices. Hopefully, if our understanding of the limitations of magnetic bearings can at least keep pace with our concept of their advantages, premature disappointment can be avoided.

To the engineer accustomed to conventional bearings, the limiting behavior of magnetic bearings will be very unfamiliar. In stark contrast to fluid film bearings, these bearings become softer (less stiff) as the shaft excursion approaches the bearing clearance. Additionally, and perhaps even more alien, the rate at which the bearing force can change is strictly limited. This phenomenon is referred to as

¹This work was supported in part by the Sundstrand Corporation Aviation Operations Division for study of aviation compressors. Partial funding was also provided by the Center for Innovative Technology of the Commonwealth of Virginia.

force slew rate limitation. Like the force slew rate, the peak force which can be generated is also subject to strict limits. These characteristics, which represent nonlinearities, are especially insistent because their onset can be quite abrupt.

Very little attention has been focused on these limitations in the literature. Britcher (ref. 1) and Sarma and Yamamura (ref. 2) have discussed operation of bearings in the magnetically saturated regime; for applications where field strength requirements are sufficiently stringent to justify the complexity of compensating for the resulting nonlinearity. Hebbale (ref. 3) presents a fairly thorough investigation of nonlinear performance in the unsaturated regime, but the study concentrates on eddy current effects in unlaminated rotors. Lamination of the rotor has become common practice and the eddy currents are readily reduced to where their contribution to nonlinear effects is minimal.

This paper represents an effort to describe some aspects of the limiting behavior of magnetic bearings and to suggest methods by which the required dynamic capacity of the bearing may be estimated.

Nomenclature

A_g	area of each air gap perpendicular to the magnetic flux	L_c	coil electrical inductance
A_p	minimum pole cross sectional area perpendicular to the magnetic flux	N	number of coil turns per pole pair
B	magnetic flux density	R_c	coil electrical resistance
B_{sat}	saturation flux density	R_f	current sensing resistance
F_x	bearing force in the x direction	t	time
F_{max}	bearing load capacity		
f	force slew rate: dF/dt	V_c	voltage across coil
g	length of the air gap	V_s	power supply voltage
G	nominal air gap: $g(x = 0)$	x	displacement of the rotor from the centered position
I_b	coil bias current: invariant	x_o	geometric clearance
i_p	coil perturbation current	β	sensitivity of the air gap to shaft displacement: $\partial g/\partial x$
K_i	magnetic actuator gain: $\partial F_x/\partial i_p$	γ	nondimensional bearing parameter
K_{nom}	nominal bearing stiffness	δ	bearing characteristic length
k_o	feedback gain: i_p/x	μ_o	magnetic permeability of air
K_x	open loop bearing stiffness	σ	nondimensional displacement: x/δ
$K_{x,cl}$	closed loop bearing stiffness	Φ	magnetic flux

Bearing Description

A wide variety of magnetic configurations has been proposed for accomplishing magnetic levitation. In applications where load capacity must be maximized relative to the size of the bearing package, the configuration described by figures 1 and 2 is the most commonly used.(refs. 3,4,5,6) For such a bearing, the force generated is a

nonlinear function of the current in the coils and the rotor displacement:

$$F_x = \frac{1}{4} \mu_0 \beta N^2 A \left[(i_1/g_1)^2 - (i_2/g_2)^2 \right] \quad (1)$$

where the gap lengths have been assumed to vary linearly with rotor displacement:

$$g_1 = G - \beta x, \quad g_2 = G + \beta x \quad (2)$$

The bearing is made to do useful work on a system by varying the currents i_1 and i_2 in a manner correlated to the rotor displacement. Various methods have been proposed for linearizing the relation between a control signal and the resulting bearing force. These include establishing a bias flux and using the control signal to perturb it (refs. 5 and 6), relating i_1 and i_2 to the square root of the control signal (ref. 5), and using feedback of the actual magnetic flux level (ref. 4). In the discussion which ensues, the bearing is assumed to be bias flux linearized. The resulting performance and nonlinearities are similar to what would be obtained with square root linearization. Flux feedback has the potential to greatly reduce flux saturation nonlinearities and eliminate softening of the bearing with large displacements. However, no actual applications of this linearization have been reported; it seems more useful to discuss the prevalent designs.

Two methods have been reported for accomplishing bias flux linearization. The more common of the two is to establish a bias current in each of the bearing coils and then modulate it by adding a perturbation current proportional to the control signal. The other scheme is functionally identical except that the bias flux is established by linking the flux from a set of permanent magnets to that of the bearing coils in the air gaps. The latter scheme is somewhat more complicated to construct but can be substantially more energy efficient. Either scheme, however, is governed by the same operating equation and is subject to the same limiting behavior.

If bias flux linearization is employed, then equation (1) can be recast as

$$F_x = \frac{\mu_0 A N^2 \beta}{4} \left[\frac{(I_b + i_p)^2}{(G - \beta x)^2} - \frac{(I_b - i_p)^2}{(G + \beta x)^2} \right] \quad (3)$$

As mentioned above, permanent magnets can be used to establish the bias flux rather than bias currents. In this case I_b would be replaced by the field strength of the permanent magnets, scaled appropriately.

Maximum Bearing Force Limits

The most immediately apparent limiting behavior of magnetic bearings is that of peak force limitation. This limitation is primarily due to nonlinearity in the magnetization curve of the electromagnet core material. Equation (1) is based on the assumption that the core magnetic flux is simply proportional to the magnetomotive force (MMF: coil turns x coil current). The actual relationship between these two quantities is depicted in the magnetization curve for the core material. Figure 3 shows a typical curve for conventional magnet iron. The significant feature is the leveling of the curve at high MMF's; beyond a certain point, the flux density ceases to increase substantially. This phenomenon is referred to as magnetic saturation and the flux density at which it occurs is the saturation flux density. Typically, this

number ranges between 1.2 and 1.6 Tesla, while some special materials push this limit slightly over 2.0 Tesla. The effect of magnetic saturation is that, once a certain coil current is reached, further increases in current will produce relatively little increase in bearing force.

The peak force which can be developed by a given magnetic bearing is determined in the following manner. The maximum flux in the most restricted cross section of the pole structure is

$$\phi_p = B_{sat} A_p \quad (4)$$

The maximum flux in each air gap of the magnetic circuit is

$$\phi_g = \mu_o N I_{sat} A_g / 2G \quad (5)$$

Since these two fluxes must be equal, equations (4) and (5) can be combined to obtain

$$N I_{sat} = 2GB_{sat} A_p / \mu_o A_g \quad (6)$$

Combining equations (6) and (3) by setting $i_p = I_b$, $I_b = \frac{1}{2} I_{sat}$, and $x = 0$ yields

$$F_{max} = \beta B_{sat}^2 A_p^2 / \mu_o A_g \quad (7)$$

It is readily shown that F_{max} is maximized by setting $I_b = \frac{1}{2} I_{sat}$. Throughout the remainder of this paper, it will be assumed that this design rule is followed.

As an example, consider a bearing designed with a pole face area of 10 cm^2 (1.6 in^2), a minimum pole cross sectional area of 7 cm^2 (1.1 in^2), and a geometry factor of 0.93. If the saturation flux density is 1.2 Tesla, equation (7) indicates that the peak force which can be developed is 524 N (118 lb).

Force Slew Rate Limits

The bearing force slew rate is limited because the magnet coils have a high inductance and the power supply to the driving amplifier is at a fixed voltage. For small displacements about $x = 0$, equation (3) can be linearized as

$$F_x = K_i i_p - K_x x \quad (8)$$

where

$$K_i = \mu_o A_g N^2 I_b \beta / G^2 \quad \text{and} \quad K_x = -\mu_o A_g N^2 I_b^2 \beta^2 / G^3 \quad (9)$$

If x is held constant so that we can investigate how rapidly the bearing force can be changed by varying the current then

$$dF_x/dt \Big|_{x=0} = K_i di_p/dt \quad (10)$$

The voltage across the electromagnet coil is

$$V_c = (I_b + i_p)R_c + L_c di_p/dt \quad (11)$$

If the output stage of the amplifier which drives the coil is described by figure 4, where it is essentially a variable resistance between the coil and ground (the resistance being variable between about 0.5 ohms and nearly infinity), then the fastest possible positive force slew rate is

$$dF_x/dt < K_i \left[V_s - (I_b + i_p)(R_c + 0.5 + R_f) \right] / L_c \quad (12)$$

For this output stage configuration, the largest negative force slew rate is determined by the reverse breakdown voltage of the output transistor. This limitation is typically larger (in magnitude) than that imposed by equation (12). Similar arguments apply to P-channel or bipolar output devices, push-pull configurations, and pulse-width-modulated amplifiers; the slew rate limitation is inherent in the fixed power supply voltage V_s .

Figure 5 illustrates this effect. The trace shown is of the coil current actually delivered to the bearing coils when the slew rate of the sinusoidal control signal exceeds the maximum slew rate permitted by the power supply voltage (200 VDC) and the coil inductance (0.95 H). Notice that the wave form is distorted only on the ascending portion. Distortion begins in the region where the positive slew rate is greatest, but is more evident as time proceeds because the current error is the time integral of the slew rate error. Once the slew rate limitation sets in, the current simply increases at the rate set by equation (12) until the demanded current and actual current once again coincide. In the case illustrated by figure 5, this occurs slightly after the peak. The descending portion of the waveform is undistorted because the reverse breakdown voltage of the output transistor (900 V) is far in excess of the 200 V power supply.

Slew rate limitation has two effects on the performance of the bearing. First, since it causes the bearing force to change more slowly than the control signal demands, it introduces phase lag. This is shown in figure 6, where the phase shift through the amplifier is plotted as a function of frequency for various power supply voltages. This produces a sudden loss of damping at high amplitudes, which can be catastrophic. The other effect is due to the asymmetry of the distortion relative to the bias level. This effectively reduces the bias current which, in accordance with equation (9), reduces the actuator gain, K_i . The result is a reduction in both stiffness and damping of the bearing.

In order to understand how to design around the force slew rate limitation, equation (12) must be examined with an eye to what the significant design parameters are. The inductance of the magnet coil is defined by

$$L_c = (N\Phi)/I \quad (13)$$

where I is the coil current required to produce a magnetic flux Φ . Equations (4), (5), (7), and (13) can be used to convert equation (12) to the form:

$$dF_x/dt < \frac{2\beta B_{sat} A_p}{\mu_o A_g N} \left[V_s - (I_b + i_p)(R_c + 0.5 + R_f) \right] \quad (14)$$

In general, the term $(I_b + i_p)(R_c + 0.5 + R_f)$ is on the order of 5% of V_s . The ratio A_p/A_g should be 1.0 for a thrust bearing ($\beta = 1$) and about 0.99 for radial bearings

($\beta \approx 0.93$). Thus the controlling design parameters are the power supply voltage and the number of coil turns. Requiring a large power supply voltage will degrade the thermal efficiency of the power amplifier which drives the bearing. However, space restrictions and thermal requirements will generally limit the usable number of coil windings. Both parameters must be carefully juggled in order to obtain adequate slew rate capacity.

Displacement Sensitivity

Displacement sensitivity of magnetic bearings is most evident as a softening of the bearing, or reduction of its spring rate, as the shaft approaches the radial clearance. This is a consequence of the nonlinear nature of equation (3). In order to readily describe this behavior, it will be assumed that the bearing has been designed to operate as a simple spring, without damping. To accomplish this, the perturbation current, i_p , is controlled by feedback of the shaft position:

$$i_p = -k_o x \quad (15)$$

The force equation (3) becomes

$$F_x = \frac{\mu_o A N^2 \beta}{4} \left[\frac{(I_b - k_o x)^2}{(G - \beta x)^2} - \frac{(I_b + k_o x)^2}{(G + \beta x)^2} \right] \quad (16)$$

The effective spring rate is the negative derivative of the bearing force with respect to deflection:

$$K_{x,cl} \equiv - \partial F_x / \partial x = \frac{\mu_o A N^2 \beta}{2} (k_o G - \beta I_b) \left[\frac{I_b - k_o x}{(G - \beta x)^3} + \frac{I_b + k_o x}{(G + \beta x)^3} \right] \quad (17)$$

Equation (17) is more tractable when nondimensionalized. To do this, two bearing characteristics are introduced: the maximum force or load capacity, F_{max} , and the nominal stiffness, K_{nom} . Noting that the nominal stiffness is that where $x = 0$,

$$K_{nom} = \mu_o A N^2 \beta I_b (k_o G - \beta I_b) / G^3 \quad (18)$$

If the bias current is half of the saturation current then the maximum force will be generated when $x = -I_b/k_o$:

$$F_{max} = \mu_o A N^2 \beta I_b k_o / (k_o G + \beta I_b)^2 \quad (19)$$

Note that equation (19) will predict a lower maximum force than will equation (7), where the maximum force was found at $x = 0$ and without defining a feedback law. Equations (18) and (19) define a characteristic length of the bearing

$$\delta \equiv F_{max} / K_{nom} \quad (20)$$

If the following nondimensional quantities are defined:

$$\gamma \equiv \beta I_b / k_o G, \quad r(\gamma) \equiv (1+\gamma)^2(1-\gamma)/\gamma, \quad \sigma \equiv x/\delta, \quad \kappa \equiv K_{x,cl} / K_{nom} \quad (21)$$

then equation (17) can be nondimensionalized as

$$\kappa = \frac{r^2}{2\gamma} \left[\frac{\gamma r - \sigma}{(r - \sigma)^3} + \frac{\gamma r + \sigma}{(r + \sigma)^3} \right] \quad (22)$$

The definitions of equation (21) lead to a useful expression for the air gap in terms of the characteristic length, δ , and the bearing parameter, γ :

$$G = \beta \delta (1+\gamma)^2(1-\gamma)/\gamma \quad (23)$$

Equation (22) is particularly useful because it describes the variation of bearing stiffness in terms of the nondimensional shaft displacement, σ , and the bearing parameter, γ , in such a way that σ and γ are entirely independent. This permits comparison of a wide variety of bearings having the same stiffness and load capacity but different clearances.

Figure 7 illustrates the family of curves defined by equation (22) for $0 \leq \gamma \leq 0.66$, $0 \leq \sigma \leq 1.0$. Stiffness curves for $\gamma = .64, .50, .40$, and $.10$ are shown separately in figure 8. The geometric requirement that $G \geq \delta$ dictates [by equation (23)] that $0 < \gamma < 0.755$. Further, since magnetic saturation sets in for $|\delta| > 1$, equation (22) is not valid for values of δ outside this range. Clearly, the bearing is most linear in the region of $\gamma = 0.5$ and as γ approaches zero. In interpreting these graphs, it is important to recognize that equation (22) implies that, as γ approaches zero, the air gap, G , becomes very large. This means that establishing the required magnetic flux in the air gap will require very high coil currents with the accompanying high I^2R power losses. Leakage flux losses are also accentuated by large air gaps.

To illustrate the use of these equations consider the design of a thrust bearing ($\beta = 1.0$) which is to have a nominal stiffness of 2×10^6 N/m (1.1×10^4 lb/in) and a load capacity of 500 N (112 lb). The characteristic length, δ , is 0.25 mm (0.010 in). If a bearing parameter, γ , of 0.5 is selected for high linearity and low I^2R losses, then the air gap would be [from equation (23)] 0.56 mm (0.022 in). At a rotor displacement of 0.20 mm (0.008 in), equation (22) predicts that the stiffness would be 88% of the nominal stiffness, or 1.8×10^6 N/m (9700 lb/in). At 0.25 mm, this figure would decrease to 64%.

Estimating Dynamic Requirements

The preceding discussion illustrates the importance of staying within the performance bounds of the magnetic bearing. Exceeding the peak force or slew rate limitations can introduce a sudden drop in bearing stiffness and damping. The resulting dynamic behavior can be disastrous. If the bearing is designed to minimize its displacement sensitivity, then it may be permissible to neglect this additional nonlinearity, especially if the design load capacity is somewhat greater than the actual dynamic requirement of the bearing. For any of these considerations, a careful assessment must be made of the actual forces that the bearing will be asked to deliver.

In estimating the dynamic requirements of a magnetic bearing, the designer may initially incline to set them equal to the worst dynamic characteristics of the anticipated loads. However, this is unrealistic and commonly demands far more performance of the bearing than is needed. In the following, two types of loads are discussed: step and sinusoidal. For the sake of simplicity, it will be assumed that the system being supported by the bearing is a simple mass. This assumption permits some fairly

general conclusions to be reached concerning slew rate and peak force requirements which will provide useful first pass design information and, more importantly, will help develop a sense of where these requirements come from. More exact estimates of the dynamic requirements placed on the bearing require detailed knowledge of the supported structure and the control algorithm.

Assume that a rigid body of mass m is supported by a control force, F_c . Because of geometric restrictions, the body cannot be permitted to move more than a distance x_0 from its unloaded position. If a step force of F_s is applied to this body, then its time trajectory is described by

$$m \frac{d^2x}{dt^2} = F_c - F_s \quad : \quad x(0) = x_0, \quad dx/dt(0) = 0 \quad (24)$$

If, further, the control force is assumed to be initially zero and then changes at a fixed slew rate of f : $F_c = ft$, then equation (22) can be solved as

$$x = ft^3/6m - F_s t^2/2m + x_0, \quad t \geq 0 \quad (25)$$

The body will collide with the geometric constraint if $x = 0$ for some $t > 0$. It can readily be shown that equation (25) has no positive real roots in t if

$$f > (2F_s^3/3mx_0)^{1/2} \quad (26)$$

For such a simple control scheme (essentially the integral of bang-bang), the peak force required of the controller is twice the applied load. If the force slew rate were unrestricted, then the peak force need be only slightly greater than F_s .

As an example, consider a body having a mass of 0.5 Kg (1.1 lbm). If the largest allowable excursion from its undisturbed position is 0.5 mm (0.020") and a step load of 100 N (22.5 lb) is applied, then a force slew rate of at least 52,000 N/sec (11,600 lb/sec) is required to prevent a collision. Figure 9 shows the time response of this system. The control algorithm used in this simulation consisted of delivering a constant force slew rate of $\pm 52,000$ N/sec or zero.

When the same system is excited by a sinusoidal force at frequency ω , then the analysis is even simpler. The best control force will obviously be sinusoidal, 180° out of phase with the load. The time response of the system is

$$x = (F_c - F_s)/(m\omega^2) \sin\omega t \quad (27)$$

The restriction that $|x| < x_0$ implies that

$$F_s - x_0 m\omega^2 < F_c < F_s + x_0 m\omega^2 \quad (28)$$

For a sinusoidal control force, the peak force slew rate is simply ω times the peak force:

$$\omega F_s - x_0 m\omega^3 < f < \omega F_s + x_0 m\omega^3 \quad (29)$$

If the same mass as in the preceding example were acted upon by a force of constant amplitude 50 N (11.2 lb) but over a frequency range of 100 rad/sec to 1000 rad/sec (955 RPM to 9550 RPM) then the control force actuator would have to be capable of delivering a force as large as 47.5 N (10.7 lb). The maximum required slew rate would occur at

$$\partial(\omega F_s - x_0 m \omega^3) / \partial \omega = 0 \Rightarrow \omega = 258.2 \text{ rad/sec}$$

Thus, the actuator must be able to provide a slew rate of 8,607 N/sec (1,934 lb/sec).

Conclusion

This paper has treated three forms of nonideal behavior found in magnetic bearings. These include peak force limitation due to magnetic saturation, force slew rate limits due to magnet coil inductance and finite power supply voltages, and displacement sensitivity due to the nonlinear dependence of the bearing force on rotor position. The mechanisms which give rise to these limitations have been explored in some detail with the purpose of developing several relatively simple equations which can be employed in the design process.

As a complement and, perhaps, to motivate this interest in bearing limitations, a very simple discussion was given of the minimum dynamic requirements made on a bearing by a sinusoidally or step excited mass. The intent here was twofold. First, it was desired to demonstrate that the dynamic requirements do not necessarily match the characteristics of the external loads. Second, this simple analysis provides some useful guidelines for estimating the requirements of actual systems.

When working with a mechanism as readily tailored as a magnetic bearing, it is easy to lose sight of its limitations. These devices present the engineer with a solution to a vast range of difficult bearing problems, but if misapplied, their performance can be very disappointing. Hopefully, this investigation will help provide methods for ensuring that magnetic bearing designs will perform as intended.

References

1. Britcher, C.P. "Progress Toward Magnetic Suspension and Balance Systems for Large Wind Tunnels". *Journal of Aircraft*, Vol. 22, No. 4, April 1985.
2. Sarma, M.S. and Yamamura, A. "Nonlinear Analysis of Magnetic Bearings for Space Technology". *IEEE Trans. on Aero. and Elec. Systems*, Vol. AES-15, No. 1, Jan. 1979.
3. Hebbale, K.V. "A Theoretical Model for the Study of Nonlinear Dynamics of Magnetic Bearings", Masters Thesis, Cornell University, Jan. 1985.
4. Kral, K.D. and Havenhill, D.D. "Magnetic Suspension and Pointing System with Flux Feedback Linearization", U. S. Patent number 4,642,501; Feb. 10, 1987.
5. Bleuler, H. "Decentralized Control of Magnetic Rotor Bearing Systems", Ph.D. Dissertation, Swiss Federal Institute of Technology, ETH report number 7573, 1984.
6. Allaire, P.E., Humphris, R.R., and Kelm, R.D. "Magnetic Bearings for Vibration Reduction and Failure Prevention". Proceedings of the 45th Meeting of the Mechanical Failure Prevention Group, April 16-18, 1985, NBS, Gaithersburg, MD.

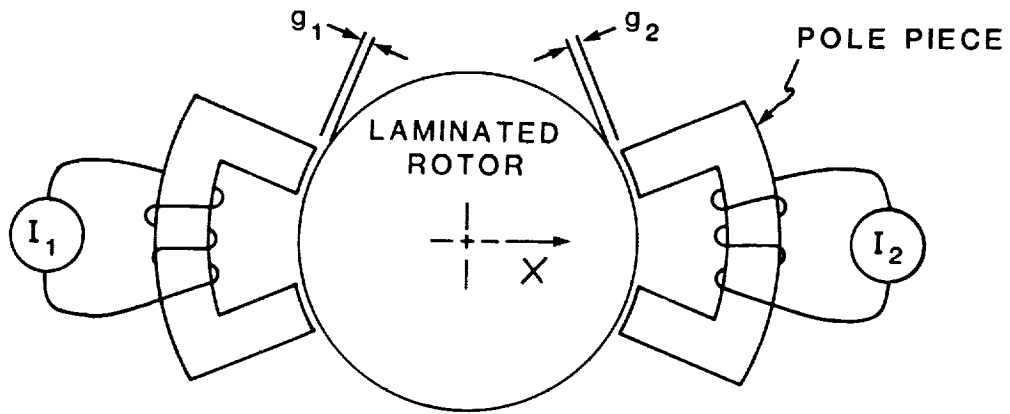


FIGURE 1. BEARING SCHEMATIC

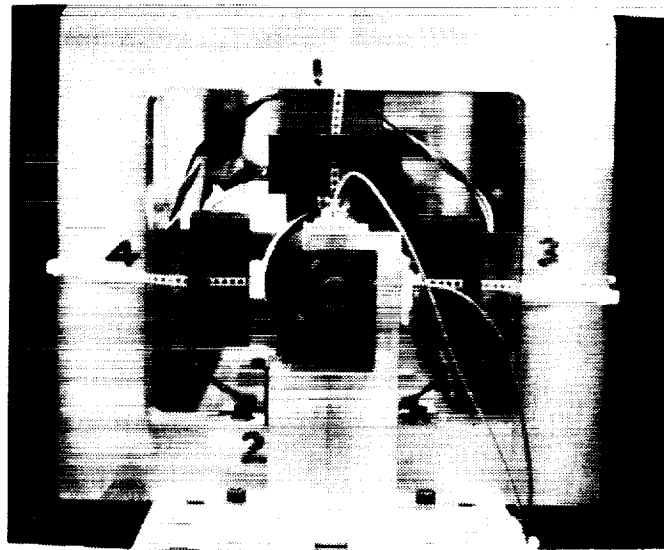


FIGURE 2. LABORATORY BEARING (ROMAC)

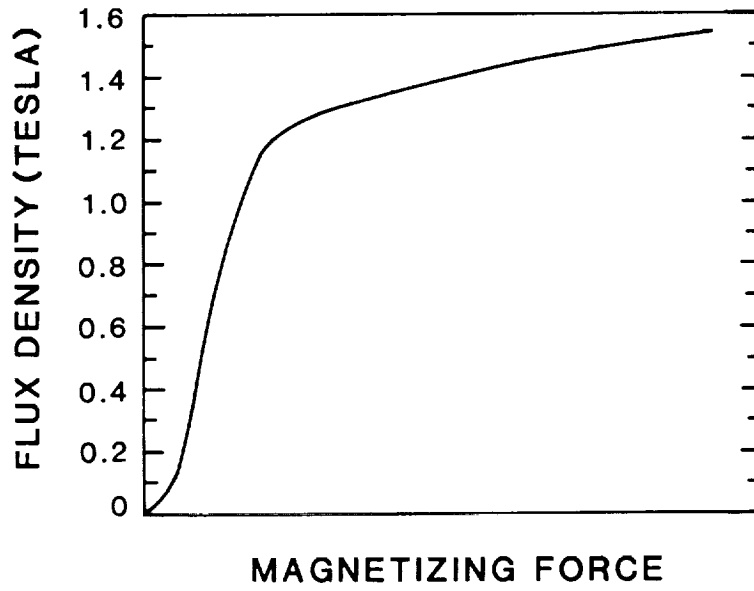


FIGURE 3. MAGNETIZATION CURVE

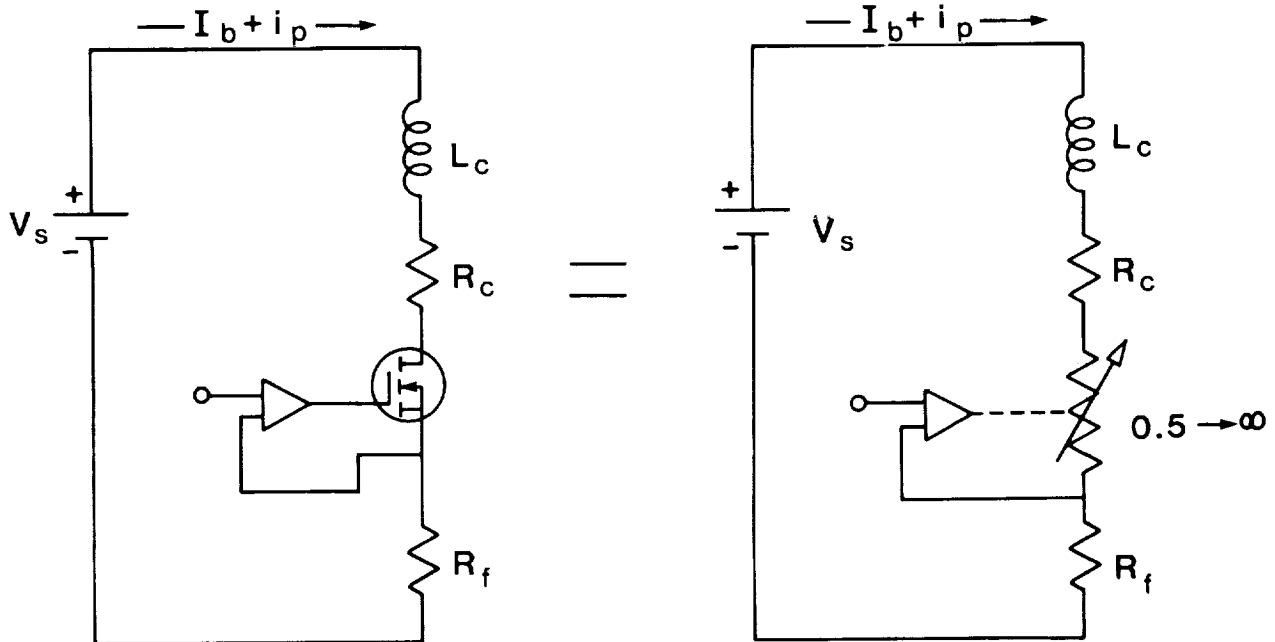


FIGURE 4. SIMPLIFIED AMPLIFIER SCHEMATIC

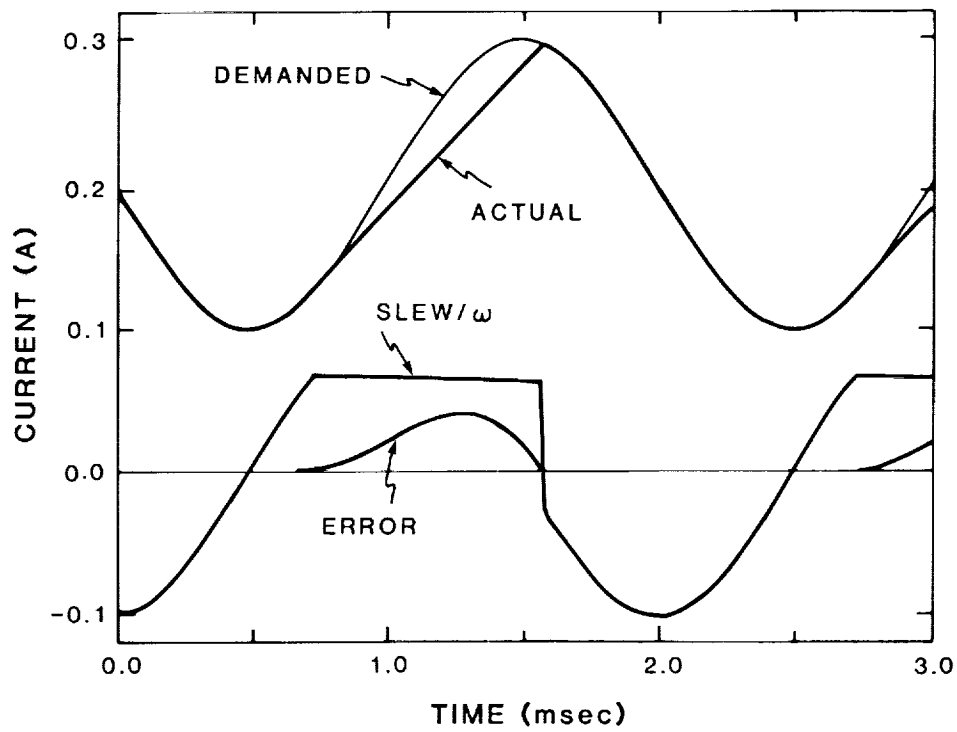


FIGURE 5. CURRENT DISTORTION DUE TO SLEW RATE LIMITATION

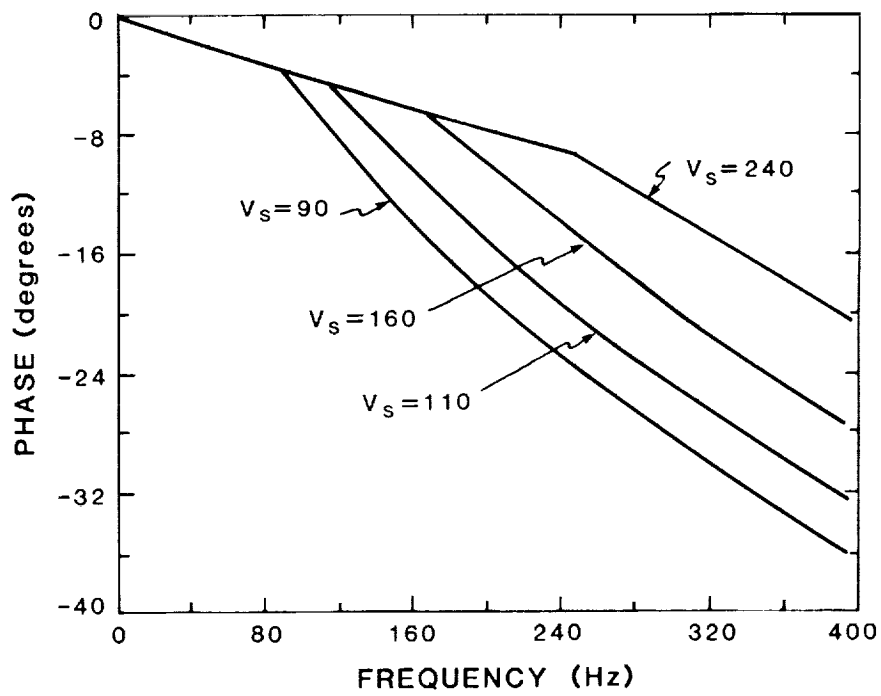


FIGURE 6. PHASE SHIFT: CONTROL SIGNAL TO COIL CURRENT

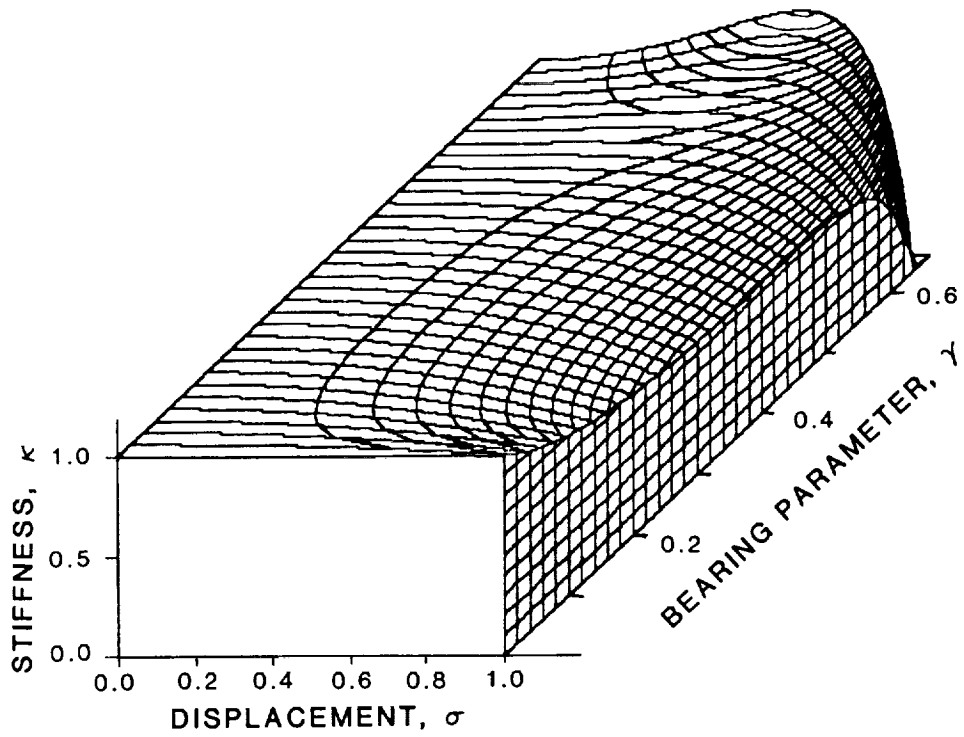


FIGURE 7. DISPLACEMENT SENSITIVITY

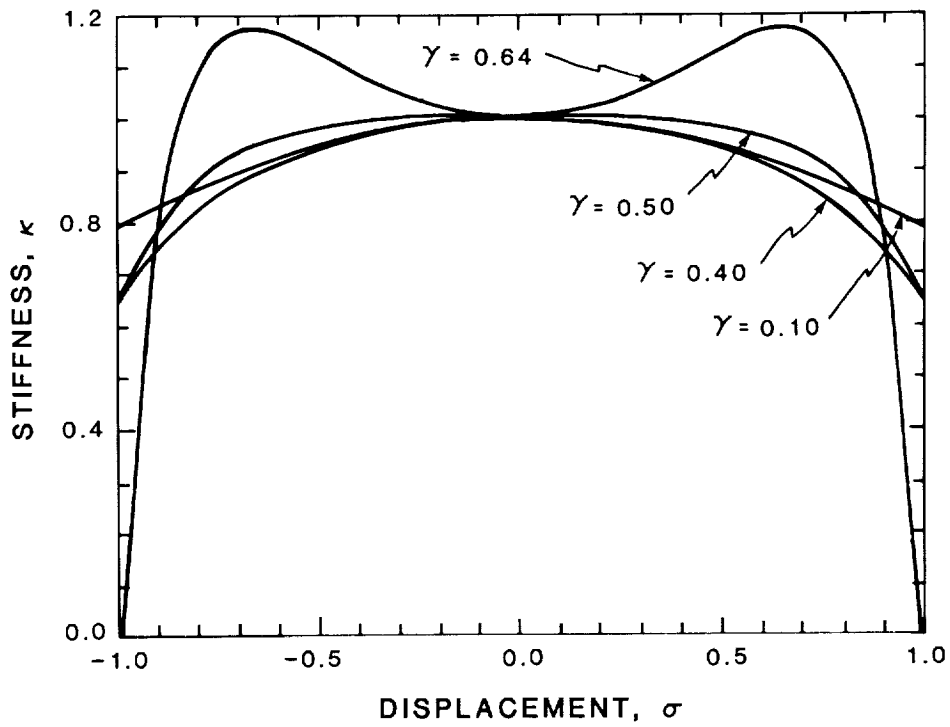


FIGURE 8. DISPLACEMENT SENSITIVITY

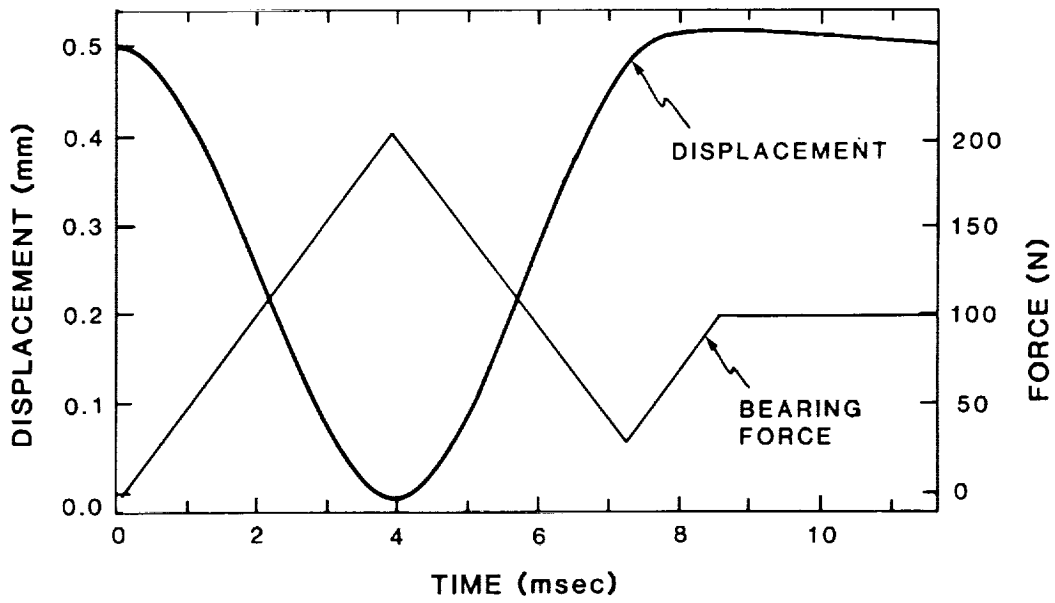


FIGURE 9. SLEW RATE LIMITED CONTROL: STEP RESPONSE